Published in final edited form as:
Arthritis Rheum. 2013 August ; 65(8): 2161–2171. doi:10.1002/art.38008.

Protein Kinase Cδ Deficiency Causes Mendelian Systemic Lupus Erythematosus With B Cell–Defective Apoptosis and Hyperproliferation

Alexandre Belot, MD, PhD[1], **Paul R. Kasher, PhD**[2], **Eleanor W. Trotter, PhD**[3], **Anne-Perrine Foray, MD, MSc**[4], **Anne-Laure Debaud, PhD**[5], **Gillian I. Rice, PhD**[2], **Marcin Szynkiewicz, MSc**[2], **Marie-Therese Zabot, PhD, PharmD**[6], **Isabelle Rouvet, PhD, PharmD**[6], **Sanjeev S. Bhaskar, MSc**[2], **Sarah B. Daly, PhD**[2], **Jonathan E. Dickerson, PhD**[2], **Josephine Mayer, MBChB, MRes**[2], **James O'Sullivan, BSc**[2], **Laurent Juillard, MD, PhD**[7], **Jill E. Urquhart, PhD, BSc (Hons)**[2], **Shameem Fawdar, PhD**[3], **Anna A. Marusiak, PhD**[3], **Natalie Stephenson, PhD**[3], **Bohdan Waszkowycz, PhD**[3], **Michael W. Beresford, MBChB, PhD**[8], **Leslie G. Biesecker, MD**[9], **Graeme C. M. Black, MD, PhD**[2], **Céline René, PhD, PharmD**[10], **Jean-François Eliaou, MD, PhD**[11], **Nicole Fabien, MD, PhD**[12], **Bruno Ranchin, MD**[13], **Pierre Cochat, MD, PhD**[14], **Patrick M. Gaffney, MD**[15], **Flore Rozenberg, MD, PhD**[16], **Pierre Lebon, MD**[16], **Christophe Malcus, PharmD, PhD**[17], **Yanick J. Crow, MD, BMedSci, MBBS, MRCP, PhD**[2], **John Brognard, PhD**[3], and **Nathalie Bonnefoy, PhD**[18]

[1]Centre de Référence des Maladies Rénales Rares, Hospices Civils de Lyon, INSERM U1111, UMS3444/US8, Université Claude Bernard Lyon 1, and Université de Lyon, Lyon, France
[2]Manchester Academic Health Science Centre and University of Manchester, Manchester, UK
[3]Paterson Institute for Cancer Research and University of Manchester, Manchester, UK
[4]Hospices Civils de Lyon, INSERM U1111, UMS3444/US8, Université Claude Bernard Lyon 1, and Université de Lyon, Lyon, France [5]INSERM U1111, UMS3444/US8, Université Claude Bernard Lyon 1, and Université de Lyon, Lyon, France [6]Centre de Biotechnologie Cellulaire, Groupement Hospitalier Est, and Hospices Civils de Lyon, Lyon, France [7]Hôpital E. Herriot, Hospices Civils de Lyon, Université Claude Bernard Lyon 1, and Université de Lyon, Lyon,

Address correspondence to: Yanick J. Crow, BMedSci, MBBS, MRCP, PhD, Genetic Medicine, University of Manchester, Manchester Academic Health Science Centre, Central Manchester University Hospitals NHS Foundation Trust, St. Mary's Hospital, Oxford Road, Manchester M13 9WL, UK (yanickcrow@mac.com); or to John Brognard, PhD, Paterson Institute for Cancer Research, University of Manchester, Wilmslow Road, Manchester M20 4BXUK, UK (JBrognard@picr.man.ac.uk); or to Nathalie Bonnefoy, PhD, Institut de Recherche en Cancérologie de Montpellier (IRCM), INSERM U896, Campus Val d'Aurelle, 34298 Montpellier Cedex 5, France (nathalie.bonnefoy@inserm.fr).
Drs. Belot, Kasher, and Trotter contributed equally to this work.

AUTHOR CONTRIBUTIONS

All authors were involved in drafting the article or revising it critically for important intellectual content, and all authors approved the final version to be published. Dr. Bonnefoy had full access to all of the data in the study and takes responsibility for the integrity of the data and the accuracy of the data analysis.

Study conception and design. Belot, Kasher, Trotter, Debaud, Bhaskar, Black, René, Eliaou, Crow, Brognard, Bonnefoy.

Acquisition of data. Belot, Kasher, Trotter, Foray, Debaud, Rice, Szynkiewicz, Zabot, Rouvet, Bhaskar, Daly, Mayer, O'Sullivan, Juillard, Urquhart, Fawdar, Marusiak, Beresford, Biesecker, René, Eliaou, Fabien, Ranchin, Cochat, Gaffney, Rozenberg, Malcus, Crow, Brognard, Bonnefoy.

Analysis and interpretation of data. Belot, Kasher, Trotter, Debaud, Szynkiewicz, Zabot, Rouvet, Bhaskar, Dickerson, O'Sullivan, Juillard, Urquhart, Stephenson, Waszkowycz, René, Eliaou, Ranchin, Cochat, Gaffney, Lebon, Crow, Brognard, Bonnefoy.

France [8]University of Liverpool, Liverpool, UK [9]NIH, Bethesda, Maryland, and NIH Intramural Sequencing Center, Rockville, Maryland [10]Centre Hospitalier Régional Universitaire de Montpellier and Université Montpellier 1, Montpellier, France [11]Centre Hospitalier Régional Universitaire de Montpellier, Institut de Recherche en Cancérologie de Montpellier (IRCM), INSERM U896, Université Montpellier 1, and Institut Régional du Cancer de Montpellier, Montpellier, Montpellier, France [12]Centre Hospitalier Lyon Sud and Hospices Civils de Lyon, Lyon, France [13]Centre de Référence des Maladies Rénales Rares and Hospices Civils de Lyon, Lyon, France [14]Centre de Référence des Maladies Rénales Rares, Hospices Civils de Lyon, Université Claude Bernard Lyon 1, Université de Lyon, and Epidemiologie Pharmacologie Investigation Clinique Information Medicale Mere Enfant (EPICIME), Lyon, France [15]Oklahoma Medical Research Foundation, Oklahoma City [16]Université Paris Descartes, Paris, France [17]Hôpital E. Herriot and Hospices Civils de Lyon, Lyon, France [18]Hospices Civils de Lyon, INSERM U1111, UMS3444/US8, Université Claude Bernard Lyon 1, and Université de Lyon, Lyon, France, and Institut de Recherche en Cancérologie de Montpellier (IRCM), INSERM U896, Université Montpellier 1, and Institut Régional du Cancer de Montpellier, Montpellier, France

Abstract

Objective—Systemic lupus erythematosus (SLE) is a prototype autoimmune disease that is assumed to occur via a complex interplay of environmental and genetic factors. Rare causes of monogenic SLE have been described, providing unique insights into fundamental mechanisms of immune tolerance. The aim of this study was to identify the cause of an autosomal-recessive form of SLE.

Methods—We studied 3 siblings with juvenile-onset SLE from 1 consanguineous kindred and used next-generation sequencing to identify mutations in the disease-associated gene. We performed extensive biochemical, immunologic, and functional assays to assess the impact of the identified mutations on B cell biology.

Results—We identified a homozygous missense mutation in *PRKCD*, encoding protein kinase δ (PKCδ), in all 3 affected siblings. Mutation of *PRKCD* resulted in reduced expression and activity of the encoded protein PKCδ (involved in the deletion of autoreactive B cells), leading to resistance to B cell receptor– and calcium-dependent apoptosis and increased B cell proliferation. Thus, as for mice deficient in PKCδ, which exhibit an SLE phenotype and B cell expansion, we observed an increased number of immature B cells in the affected family members and a developmental shift toward naive B cells with an immature phenotype.

Conclusion—Our findings indicate that PKCδ is crucial in regulating B cell tolerance and preventing self-reactivity in humans, and that PKCδ deficiency represents a novel genetic defect of apoptosis leading to SLE.

Systemic lupus erythematosus (SLE) is a multi-system autoimmune disease characterized by the production of autoantibodies against nucleic acids and associated nuclear proteins (1). Juvenile-onset SLE accounts for 15–20% of all cases of lupus. The development of SLE in childhood and adolescence is typically associated with greater disease activity at the time of diagnosis, greater disease severity and associated damage over time, a relatively high male-

to-female sex ratio (2), and differences in the frequency of expression of an interferon signature in comparison with adult-onset lupus (3). Considering the shorter exposure time to putative environmental triggers, genetic factors may be relatively more important in the pathogenesis of juvenile-onset SLE (4,5). Monogenic cases of juvenile-onset SLE or SLE-like phenotypes due to mutations in complement system genes *(C1QA, C1QB, C1QC, C4A, C4B, C2*) (6), *ACP5* (7,8), *TREX1* (9), and *DNASE1L3* (10) have been reported.

Although many molecular pathways and cell types can be dysregulated in SLE, B cells have emerged as key players in disease causation through their capacity to produce pathogenic autoantibodies and immunoregulatory factors, together with their contribution to lymphoid tissue organization (11). The random nature of B cell receptor (BCR) diversification determines that a large number of BCRs will recognize self antigens. Such potentially harmful B cells are eliminated at various steps of B cell development, and a failure to select against self-reactive lymphocytes can lead to tolerance breakdown and autoimmunity (12,13). The molecular definition of autoimmune lymphoproliferative syndrome (ALPS) previously established that defective apoptosis can lead to autoimmunity in humans. Unlike the corresponding mouse model, SLE is uncommon in patients with ALPS. To date, there has been only a single report of a *FASLG* mutation in a patient with SLE and lymphoproliferative disease (14).

SLE represents a paradigm autoimmune disease that results from a breakdown of tolerance to self antigens, and B cell checkpoint impairment may contribute to development of the lupus autoimmune phenotype. Protein kinase C δ (PKCδ) is a serine/threonine kinase that has been implicated in the control of cell proliferation and apoptosis (15). Mice deficient in PKCδ develop features consistent with SLE and demonstrate a defect in the negative selection of self-reactive B cells and an expansion of peripheral B cells (16,17). Here, we describe 3 siblings from 1 kindred, all of whom fulfilled the American College of Rheumatology (ACR) criteria for a diagnosis of SLE (18). All 3 patients were homozygous for a missense mutation in *PRKCD*, the gene encoding PKCδ, resulting in the substitution of an evolutionarily invariant glycine for a serine. This mutation results in a reduction in PKCδ expression and activity. We demonstrate that PKCδ deficiency is a novel cause of Mendelian juvenile-onset SLE, in which resistance of B cells to BCR− and Ca^{2+}-dependent apoptosis is associated with increased B cell proliferation.

PATIENTS AND METHODS

Patients

Clinical details of this family have been reported previously (19), and additional information is shown in Table 1. The siblings were born to a consanguineous couple of northern European extraction. Both parents were completely healthy, and there was no history of autoimmunity in the extended family. The 3 patients are fully described in Supplementary Methods, available on the *Arthritis & Rheumatism* Web site at http://onlinelibrary.wiley.com/doi/10.1002/art.38008/abstract. Written informed consent was obtained for data collection, blood sampling, and genetic testing relating to patients, family members, and healthy control subjects. The study was approved by the Leeds (East) Multi-centre Research Ethics Committee and the Comité de Protection des Personnes Sud-EST IV.

Single-nucleotide polymorphism (SNP) mapping, sequence capture, and sequencing

Genome-wide scans were performed in subjects V-1, V-2, V-3 and V-4. Genotypes were generated using the Affymetrix Gene Chip Genome-Wide Human SNP Array 6.0. Data sets were collated and standardized to a single recent genome build (GRCh37/hg19) using the SNPsetter program (http://dna.leeds.ac.uk/snpsetter/), and the combined data were analyzed using AutoSNPa (http://dna.leeds.ac.uk/autosnpa/). Linkage analysis was performed assuming autosomal-recessive inheritance with a disease allele frequency of 0.001, complete penetrance, and an equal frequency for marker alleles. Logarithm of odds (LOD) scores were calculated using a Merlin linkage package (http:www.sph.umich.edu/csg/abecasis/Merlin).

For whole-exome analysis, targeted enrichment and sequencing were performed on 3 μg of DNA extracted from the peripheral blood of subject V-1. Enrichment was undertaken using SureSelect Human All Exon Kit version 2 (Agilent) for an Applied Biosystems SOLiD System. Electronic polymerase chain reaction (PCR) was conducted on the resultant sample library, which was then sequenced on a SOLiD 4 System (Life Technologies). Sequence data were mapped using SOLiD BioScope software (Life Technologies) and GRCh37/hg19 Human Genome as a reference. SNPs were called using the diBayes tool in the BioScope software suite with the medium stringency setting and then filtered for those SNPs with less than 5× coverage. A total of 78% of reads mapped uniquely to the genome reference, with 75% of the targeted exome covered 10-fold or higher. On average, a total of 82-fold coverage was achieved across the exome (see Supplementary Table 1, available on the *Arthritis & Rheumatism* Web site at http://onlinelibrary.wiley.com/doi/10.1002/art.38008/abstract). Mutation screening of *PRKCD* was performed by PCR amplification of genomic DNA segments and direct sequencing of the products using BigDye Terminator chemistry and a 3130 Sequencer (Applied Biosystems). Mutation descriptions are based on the reference complementary DNA (cDNA) sequence ENST00000330452, with the ATG initiation site situated at the beginning of exon 3 and the termination codon in exon 19.

Protein expression

Transient transfections of HEK 293T and H157 cell lines were carried out using Effectene reagents (Qiagen). After transfection, cells were lysed in buffer 1 (50 mmoles/liter disodium hydrogen phosphate [pH 7.5], 1 mmole/liter sodium pyrophosphate, 20 mmoles/liter sodium fluoride, 2 mmoles/liter EDTA, 2 mmoles/liter EGTA, 1% sodium dodecyl sulfate [SDS], protease inhibitor cocktail [Roche]), and lysates were separated on 12% SDS–polyacrylamide gels (Bio-Rad). For lymphoblastoid cell lines (LCLs), whole cell lysates were prepared using 10 m*M* EDTA–radioimmunoprecipitation assay buffer containing protease inhibitors (Roche). Protein expression was analyzed by Western blotting using the antibodies and concentrations described below.

Antibodies to PKCδ, phospho-PKCδ(T507), phospho-PKCδ(S645), phospho-PKC (pan) (βII Ser662), and phospho-MARCKS (S152/156) were purchased from Cell Signaling Technology (all used at 1:1,000 dilution). The antibody to phospho-MARK2 (T595) (1:1,000) was purchased from Abcam, and antibodies to tubulin (1:1,000) and to β-actin (1:14,000) were purchased from Sigma. Horseradish peroxidase–labeled goat anti-rabbit IgG

or goat anti-mouse IgG was purchased from Cell Signaling Technology. Signal was detected using Pierce ECL Western Blotting Substrate. For phorbol myristate acetate (PMA) treatment, cells were treated with 500 n*M* PMA (Promega) 24 hours after transfection and lysed after 1 minute or 5 minutes. The protein sequence of human PKCδ has a length of 676 residues, compared with a length of 674 residues in mice. This is attributable to the presence of 2 additional residues at amino acid positions 305 and 306 in humans. A nomenclature discrepancy between these 2 commonly used sequences exists in the literature, where, for example, Tyr^{313} can be referred to as Tyr^{311} and vice versa. To avoid any confusion relating to this matter in the current study, we refer to the numbering of residues based only on the human sequence.

Structural modeling

Homology modeling of the PKCδ tyrosine kinase domain structure was based on the crystal structure of PKCθ (PDB 1XJD; 73% homologous over this domain) and performed using Schrodinger Suite 2012/Maestro9.3.5.

Cloning and mutagenesis

Mutagenesis was carried out on a full-length PKCδ shuttle clone (IOH26352; Invitrogen Ultimate Open Reading Frame) using a QuikChange Site-Directed Mutagenesis Kit (Agilent) to generate G510S, K378M, and D491A by making the respective nucleotide changes. The primers used are as follows: for G1528A, forward 5′-CCAGCACCTTCTGCAGCACCCCTGACTAT-3′, reverse 5′-ATAGTCAGGGGTGCTGCAGAAGGTGCTGG-3′; for A1472C, forward 5′-CCACATCAAGATTGCCGCCT-TTGGGATGTGCAAAG-3′, reverse 5′-CTTTGCACATCCC AAAGGCGGCAATCTTGATGTGG-3′; for A1133T, forward 5′-GAGGAGAGTACTTTGCCATCATGGCCCTCA-AGA-3′, reverse 5′-TCTTGAGGGCCATGATGGCAAAGT-ACTCTCCTC-3′. Clones were transferred to a hemagglutinin destination vector using Gateway LR Clonase II (Invitrogen).

Reverse transcriptase–PCR (RT-PCR)

RT-PCR was performed using a Qiagen OneStep RT-PCR Kit according to the manufacturer's protocol. An RNeasy Mini Kit (Qiagen) was used to extract RNA from patient LCLs and a wild-type 293T cell line. Twenty nanograms of RNA was used for each reaction. The cycling conditions for PCR were as follows: cDNA synthesis and predenaturation (1 cycle at 50°C for 30 minutes followed by 95°C for 15 minutes), PCR amplification (28 cycles of denaturing at 95°C for 30 seconds, annealing at 55°C for 30 seconds, and extension at 68°C for 60 seconds), and a final extension at 72°C for 10 minutes. The PCR products were electrophoresed on 1% agarose gels and visualized with ethidium bromide under ultraviolet light. Primers for *PRKCD* were synthesized by Eurofins MWG Operon, and primers for *GAPDH* were synthesized by Integrated DNA Technologies. The sequences of these primers are as follows: for *PRKCD1* (648 bp), forward 5′-TCTGTGCCGTGAAGATGAAG-3′, reverse 5′-CAACTACATGAGCCCCACCT-3′; for *PRKCD*2 (429 bp), forward 5′-GCCTCAACAAGCAAGGCTAC-3′, reverse 5′-CAGCAACTCCGGTCTTCTTC-3′; for *GAPDH* (668 bp), forward 5′-

CCATGGAGAAGGCTGGGG-3′, reverse 5′-CAAAGTTGTCATGGATGACC-3′. The RT-PCR products were purified by gel extraction, and the sequence was confirmed by Sanger sequencing for 293T cells.

B cell purification

Blood samples were obtained from the Etablissement Français du Sang (healthy adult donors) or from patients and their family members. Peripheral blood mononuclear cells (PBMCs) were isolated by Ficoll (Eurobio) density-gradient centrifugation, and lymphocytes were then isolated by Percoll (GE Healthcare) density-gradient centrifugation. B cell enrichment was performed by negative selection using magnetic beads, according to the manufacturer's recommendations (EasySep Human B Cell Enrichment Kit; StemCell Technologies). The purity of isolated CD19+ B cells was always >95%, as determined by flow cytometry. Purified B cells were cultured in RPMI 1640 (Life Technologies) supplemented with 10% (volume/volume) heat-inactivated fetal calf serum (Lonza), 10 m*M* HEPES pH 7.5 (Life Technologies), 2 m*M* glutamine (Life Technologies), and 0.04 mg/ml gentamycin (Life Technologies).

LCL generation

LCLs were generated (CBC Biotec Centre de Ressource Biologique, Hospices de Lyon) from the PBMCs of family members by ex vivo infection with a laboratory strain of Epstein-Barr virus (B 95-8 cell line), using a standard protocol (20) and belong to the collection MAI-Lupus. Cells were maintained in RPMI 1640 (Life Technologies) supplemented with 12% heat-inactivated fetal calf serum (Lonza), 10 m*M* HEPES pH 7.5, 2 m*M* glutamine, 0.04 mg/ml gentamycin, and 0.250 mg/ml fungizone (all from Life Technologies) at 37°C in a humidified atmosphere of 5% CO_2.

Proliferation assay

To assess cell division, 2×10^5 cells were incubated with 10 μM 5,6-carboxyfluorescein di-acetate succinimidyl ester (CFSE; Molecular Probes) for 12 minutes at 37°C and then washed twice in cold culture medium. Cells were resuspended in culture medium supplemented with 2.5 μg/ml anti-F(ab′)$_2$ (Jackson Immuno-Research), 1 μg/ml CD40L in the presence of 1 μg/ml enhancer (Enzo Life Sciences), and 2.5 μg/ml of CpG oligodeoxy-nucleotide 2006 (5′-TCGTCGTTTGTCGTTTTGTCGTT-3′) complete phosphorothioate (gram molecular weight [GMW]). After 96 hours of culture, CFSE staining was assessed on a FACSCalibur flow cytometer (BD Biosciences), and data were analyzed with FlowJo software (Tree Star).

Apoptosis assay

The viability of primary CD19+ B cells or LCLs cultured in the presence of medium alone, 2.5 μg/ml of the Toll-like receptor 9 (TLR-9) ligand CpG 2006 (GMW), or 10 μM thapsigargin (an endoplasmic reticulum pump inhibitor that induces Ca^{2+} influx; Sigma) was evaluated by labeling with a combination of propidium iodide and fluorescein isothiocyanate (FITC)–conjugated annexin V (BD Biosciences) and analyzed by flow cytometry and FlowJo software.

Flow cytometric analysis

The percentages of transitional, pre-naive, naive, and memory B cell subpopulations were determined by flow cytometry, as previously described (13,20). Phycoerythrin (PE)–conjugated anti-CD24, PerCP–Cy5–conjugated anti-CD38, PE–Cy7–conjugated anti-CD19, and allophycocyanin–conjugated anti-CD5 were obtained from Beckman Coulter, FITC-conjugated anti-CD27 and PE-conjugated anti-CD20 were obtained from BD Biosciences, and PE-conjugated anti-human IgD was purchased from Dako. Stained cells were washed in phosphate buffered saline, fixed in 1% paraformaldehyde, and analyzed within 24 hours. Samples were acquired on a FACSAria II flow cytometer, and cells with the light scatter properties of lymphocytes were analyzed using FACSDiva software (BD Biosciences). As shown in Supplementary Figure 1 (available on the *Arthritis & Rheumatism* Web site at http://onlinelibrary.wiley.com/doi/10.1002/art.38008/abstract), the percentages of transitional B cells were determined by flow cytometry following labeling with PE-conjugated anti-CD20, FITC-conjugated anti-CD24, and PerCP–Cy5–conjugated anti-CD38 (BD Biosciences). Data were acquired on a FACSCalibur flow cytometer (BD Biosciences) and analyzed with FlowJo software.

Phenotypic rescue experiments in LCLs

Lentiviral infections were performed in 24-well plates seeded with 0.2×10^6 cells in the presence of 8 μg/ml Polybrene solution. LCLs established from subjects V-1 and V-2 were transduced with pLenti6.3/V5-DEST-PKCδG510S or wild-type pLenti6.3/V5-DEST-PKCδ. Plates were centrifuged at 1,800 revolutions per minute for 100 minutes at 37°C. Cells were then resuspended in complete RPMI 1640 culture medium and cultured for 7 days before blasticidin (Sigma-Aldrich) was added to the medium at a concentration of 0.01 mg/ml. The resulting stable infected cell lines were maintained in culture medium supplemented with blasticidin. PKCδ expression in transduced LCLs was determined by Western blotting.

B cell clonality and B cell repertoire

B cell clonality and B cell repertoire assessments were performed according to standard methods, which are described in detail in Supplementary Methods, available on the *Arthritis & Rheumatism* Web site at http://onlinelibrary.wiley.com/doi/10.1002/art.38008/abstract.

Statistical analysis

A nonparametric Mann-Whitney U test was used for comparisons between groups, and variations between experimental conditions were assessed with Wilcoxon's matched pairs test. Graphing and analysis of significance were performed using GraphPad Prism software. *P* values less than 0.05 were considered significant.

RESULTS

Clinical description of the patients with SLE

The siblings were born to a consanguineous couple (Figure 1A) of northern European extraction. All patients fulfilled the ACR 1982 revised criteria for the classification of SLE. Lupus rash and lupus nephritis were observed in all 3 patients (Figure 1B). Subject V-3

presented initially with transient symptoms consistent with ALPS (i.e., transient hepatosplenomegaly and lymph-adenopathy) and subsequently developed other features consistent with a diagnosis of SLE. None of the patients experienced a severe early-onset infection. Both parents were completely healthy, and there was no history of autoimmunity in the extended family. Thus, we hypothesized that the familial disorder was most likely inherited as an autosomal-recessive trait.

Homozygous mutation in *PRKCD* revealed by targeted exome sequencing

Genome-wide SNP scans performed in subjects V-1, V-2, V-3, and V-4 identified a single region of homozygosity of >1.5 Mb in size that was shared by the 3 affected individuals (V-1, V-3, and V-4) and was not observed in the unaffected sibling (V-2). Linkage analysis of this region on chromosome 3p21 (rs7650998; 46,607,255 – rs864623; 55,735,226) yielded a LOD score of 2.4. Whole-exome capture was performed by in-solution hybridization and massively parallel sequencing of DNA from subject V-1. Approximately 5 Gb of sequence was generated such that >75% of the coding bases of the GENCODE-defined exome were represented by at least 10 reads (see Supplementary Table 1, available on the *Arthritis & Rheumatism* Web site at http://onlinelibrary.wiley.com/doi/10.1002/art.38008/abstract).

PRKCD was highlighted as 1 of only 2 genes demonstrating a homozygous nonsynonymous variant (c.1528G>A; p.G510S) within the putative 5-Mb candidate disease gene interval on chromosome 3p21 using this calling strategy. Sanger sequencing confirmed only the *PRKCD* variant, which was present in the homozygous state in all 3 affected patients (Figure 1C). Both parents were heterozygous for the variant, and the unaffected sibling was wild-type homozygous. The G510 residue is highly conserved to yeast in PKCδ orthologs (Figure 1D) and sits within the activation loop of PKCδ (Figure 1E). This amino acid is also invariant within the AGC kinase family (Figure 1F). The c.1528G>A substitution was not annotated in the dbSNP (http://www.ncbi.nlm.nih.gov/projects/SNP/), ClinSeq (http://www.genome.gov/20519355) and 1000 Genomes project databases (http://browser.1000genomes.org/index.html) nor in 13,006 control chromosomes typed for this allele on the Exome Variant Server (http://evs.gs.washington.edu/EVS/). SIFT analysis classifies the c.1528G>A change as deleterious (score of 0) (http://sift.jcvi.org/), while PolyPhen annotates the mutation as “probably damaging” (score of 1.0) (http://genetics.bwh.harvard.edu/pph2/). In addition, x-ray modeling of PKCδ predicts that the glycine-to-serine substitution will result in a disruption of the activation loop of the protein (Figure 1G). To identify other SLE patients with mutations in *PRKCD*, we sequenced coding exons and conserved intron/exon boundaries of *PRKCD* in 230 affected individuals but did not identify any likely pathogenic variants (data not shown).

Activity and stability of mutant PKCδ

Expression of G510S mutant PKCδ in HEK 293T and H157 cells indicated that the mutant protein could not be phosphorylated at the activation loop (T507) (Figure 2A), resulting in an expected decrease in phosphorylation at the turn motif (S645) and the hydrophobic motif (S662) (Figure 2A). Comparable reductions were observed for the kinase-inactive mutants K378M and D491A (see Supplementary Figure 2, available on the *Arthritis & Rheumatism*

Web site at http://onlinelibrary.wiley.com/doi/10.1002/art.38008/abstract). Phosphorylation at these sites is required for activation of PKCδ (21). Consistent with these observations, the mutant protein was inactive under basal conditions and refractory to activation by the conventional PKC agonist phorbol myristate acetate, because there were no observable increases in phosphorylation of the downstream substrates MARCKS and Mark2 (Figures 2A and B). The absence of phosphorylation of PKCδ resulted in loss of protein stability, so that mutant PKCδ was degraded at a faster rate than wild-type protein (Figure 2C), while RNA expression was not altered (Figure 2D). Concordant with these data, all 3 patients homozygous for the G510S mutation expressed notably less PKCδ compared with their wild-type and heterozygous relatives (Figures 2E and F). Patient cells also demonstrated reduced phosphorylation at the T507, S645, and S662 sites, as well as a lack of activation of Mark2, the downstream target of PKCδ (Figure 2G).

Association of the *PRKCD* mutation with a shift from a B cell to an immature B cell phenotype

Lymphocyte counts for subjects V-1, V-3, and V-4, who were homozygous for the G510S mutation, were normal at the time of disease onset, with a normal proportion of B, T, and natural killer cells. However, subjects V-1 and V-4 presented with an increased number of immature CD19+CD21− B cells (Table 1). The number of transitional (CD19+CD24^{high}CD38^{high} or CD19+ IgD+CD38^{high}) B cells was also repeatedly shown to be increased in patient V-4 (Figures 3A, 3B, and Supplementary Figure 2 [available on the *Arthritis & Rheumatism* Web site at http://onlinelibrary.wiley.com/doi/10.1002/art.38008/abstract]). Similar measurements were not possible in subject V-1 because of ongoing lympho-cytopenia (and because additional samples from subject V-3 were not available). Mature IgD+CD38− B cells from patient V-4 still expressed CD5, a recognized marker of immature B cells (Figure 3B). Interestingly, heterozygous mature B cells displayed intermediate labeling for CD5, suggesting that PKCδ is required for complete mature naive B cell differentiation.

We also observed a noticeable decrease in the number of CD19+CD27+IgD+ and CD19+CD27+ IgD− memory B cells in subject V-4 but not in his mother (subject IV-1), who is a heterozygous carrier (Figure 3C). An assessment of the B cell repertoire demonstrated polyclonality with restricted diversity (48%) (see Supplementary Figure 3, available on the *Arthritis & Rheumatism* Web site at http://onlinelibrary.wiley.com/doi/10.1002/art.38008/abstract). T cell proliferative responses to either polyclonal or specific antigens were normal, immunoglobulin levels were within reference values in all cases (Table 1), and ABO iso-hemagglutinins and vaccine responses were normal in subject V-4 (data not shown).

Association between PKCδ deficiency and increased B cell proliferation

When investigating B cell responses, we observed that freshly isolated primary CD19+ B cells from subject V-4 were highly susceptible to spontaneous cell death; this effect was not generally observed in B cells from patients with juvenile-onset SLE that expressed wild-type PKCδ and had received similar treatment. Importantly, the TLR-9 ligand CpG, which is known to directly activate B cells, totally protected subject V-4–derived B cells from

spontaneous apoptosis (Figure 4A). These results suggested that B cells with mutated PKCδ were highly responsive to B cell stimuli. Supporting this hypothesis, we observed hyper-proliferative responses in peripheral B cells from subject V-4 as well as from his heterozygous carrier mother (IV-1) in response to BCR, CD40, and TLR-9 stimulation, compared with B cells from healthy control subjects or patients with juvenile-onset SLE (Figure 4B and Supplementary Figure 4 [available on the *Arthritis & Rheumatism* Web site at http://onlinelibrary.wiley.com/doi/10.1002/art.38008/abstract]).

PRKCD mutant LCLs are resistant to apoptosis and are rescued by coexpression of the wild-type protein

Together with stromal interaction molecule 1 (STIM-1) and RasGRP, PKCδ was recently shown to control a Ca^{2+}-mediated apoptotic pathway in B cells (22). In agreement with these data, primary B cells from subject V-4 as well as from his heterozygous mother (IV-1) were resistant to Ca^{2+}-dependent apoptosis induced by thap-sigargin stimulation (Figure 4C). Consistent with a disturbance in Ca^{2+}-mediated apoptosis in PKCδ mutant B cells, we demonstrated that LCLs established from mutant PKCδ carriers were more resistant to both BCR− or thapsigargin-induced apoptosis than were LCLs established from wild-type subject V-2 (Figures 4D and E). The percentage of specific apoptosis was quantified as follows: BCR− or thapsigargin-induced relative percentage cell loss = (1 − [% viable cells after treatment/% viable cells without treatment]) × 100. Expression of wild-type PKCδ in LCLs from subject V-1 rescued sensitivity to Ca^{2+}-dependent apoptosis, while the expression of G510S mutant PKCδ in LCLs derived from subject V-2 significantly decreased apoptosis (Figure 4F). Because we previously reported overexpression of the antiapoptotic molecule Bfl-1 in B cells from affected patients in this family (19), we assessed whether PKCδ modulates Bfl-1 expression but did not observe any dysregulation in LCLs from patients (data not shown).

DISCUSSION

B cell ontogenesis is tightly regulated to maintain immune tolerance and homeostasis. SLE represents a paradigmatic autoimmune disease resulting from a breakdown of tolerance to self antigens, and impairment of the B cell tolerance checkpoint may contribute to development of the lupus autoimmune phenotype. Here, we report that a homozygous *PRKCD* mutation causes a novel monogenic, autosomal-recessive form of juvenile-onset SLE and show that PKCδ regulates human B cell apoptosis and proliferation.

The PKC family comprises 11 closely related isoforms and has been implicated in a wide variety of cellular processes, including cell growth, differentiation, and apoptosis (23). Mice lacking PKCδ acquire features of SLE characterized by an expansion of the immature B lymphocyte population with the formation of numerous germinal centers, autoreactive antibodies, immune complex–associated glomerulonephritis, and lymphocyte infiltration in multiple organs (16,17). Adoptive transfer experiments suggest that this hyperproliferative phenotype is B cell autonomous.

In 3 siblings with juvenile-onset SLE, we identified a homozygous missense mutation (c. 1528G>A) in *PRKCD* that results in the substitution of an evolutionarily invariant glycine

for a serine (p.G510S). This mutation leads to reduced PKCδ expression and activity. Reinforcing a key role for PKCδ in the control of B cell proliferation, we observed an increased number of circulating transitional B cells in the peripheral blood of an affected patient. Moreover, mutant primary B cells, from both a homozygous patient and a heterozygous carrier, exhibited a higher rate of proliferation following stimulation through BCR, CD40, and TLR-9 compared with wild-type B cells.

The molecular mechanisms by which self antigen exposure leads to editing, apoptosis, or anergy at different stages of B cell development are incompletely understood. It was recently shown that PKCδ plays a crucial role in B cell negative selection through the regulation of antigen-induced proapoptotic Ras/ERK signaling (22). This pathway requires PKCδ and the guanine nucleotide exchange factor RasGRP for activation of ERK and depends on the concentration of the Ca^{2+} sensor STIM-1, which controls the magnitude of Ca^{2+} entry. Developmental regulation of these proteins was associated with selective activation of this proapoptotic pathway in transitional B cells and was impaired in PKCδ-deficient mice. Adding to the findings by Limnander et al (22), we demonstrate that B cells expressing mutated PKCδ have reduced Ca^{2+}-dependent apoptosis, thus suggesting that PKCδ is also involved in the negative selection of human B cells. ALPS is another inherited disorder characterized by defective lymphocyte apoptosis involving the Fas apoptotic pathway. Unlike the corresponding mouse model, features of SLE are very uncommon in human ALPS, with only a single such patient reported so far (14). In contrast, our 3 patients presented with an unequivocal diagnosis of SLE.

We have identified a missense mutation in *PRKCD*, the effect of which is not possible to predict a priori. In some assays, we observed what appeared to be a cellular phenotype in heterozygous carriers. However, the (heterozygous) parents of our patients remain healthy, and no family history of autoimmune disease exists. Thus, clinically, the disease behaves as a recessive trait. The reason for this remains uncertain but might relate to a threshold effect. We make the point here that the possibility of an attenuated/late-onset phenotype in heterozygotes cannot be ruled out.

Reminiscent of observations in PKCδ-deficient mice, we observed an increased number of immature B cells in a homozygous patient, with an expansion of peripheral transitional B cells. Furthermore, CD5 was increased in the naive mature B cells of patient V-4, which is suggestive of a defect in early B cell tolerance checkpoints. Thus, the restricted B cell repertoire of subject V-4 could be linked to altered BCR signaling and persistence of CD5 expression on B cells (24). Of note, in contrast to the reported consequences of mutations in *STIM1* (25), none of our patients presented with features of early-onset immunodeficiency. This finding suggests that PKCδ plays a restricted role in BCR− and Ca^{2+}-dependent signaling.

To date, the definition of monogenic causes of SLE has highlighted 2 major molecular pathways involved in human immunologic tolerance: disturbed clearance of apoptotic material and up-regulated production of type I interferon. The *PRKCD* mutation described here represents an additional Mendelian cause of disturbed apoptosis coupled to dysregulated B cell proliferation, leading to SLE in humans. This reinforces recent emerging

data indicating that transitional B cells are an important cell type in the pathogenesis of lupus (26,27).

Acknowledgments

Supported by specific funding from the Hospices Civils de Lyon, the Réseaux Thématiques de Recherche Translationelle INSERM, the Fondation pour la Recherche Médicale, the Région Rhone-Alpes, and the Société Française de Rhumatologie (all to Dr. Belot) and by institutional grants from INSERM and Université de Lyon (to Dr. Bonnefoy). Dr. Gaffney's work was supported by the NIH (grants RC2-AR-058959 and R01-AI-063274). Dr. Brognard's work was supported by Cancer Research UK (grant C5759/A12328). Work performed in the Crow laboratory contributing to this research received funding from the European Union Seventh Framework Programme (FP7/2007–2013 project NIMBL; 241779).

We would like to thank the family members for their cooperation with the research presented here, and Nadia Plantier (ImmunID Technologies) for helpful discussions. Dr. Crow acknowledges the NIHR Manchester Biomedical Research Centre. Dr. Bonnefoy acknowledges the Plateforme de Cytométrie en Flux of SFR Biosciences Gerland-Lyon Sud (UMS344/US8) for their technical assistance.

References

1. Rahman A, Isenberg DA. Systemic lupus erythematosus. N Engl J Med. 2008; 358:929–39. [PubMed: 18305268]
2. Brunner HI, Huggins J, Klein-Gitelman MS. Pediatric SLE: towards a comprehensive management plan. Nat Rev Rheumatol. 2011; 7:225–33. [PubMed: 21386795]
3. Bennett L, Palucka AK, Arce E, Cantrell V, Borvak J, Banchereau J, et al. Interferon and granulopoiesis signatures in systemic lupus erythematosus blood. J Exp Med. 2003; 197:711–23. [PubMed: 12642603]
4. Crow YJ. Lupus: how much "complexity" is really (just) genetic heterogeneity? Arthritis Rheum. 2011; 63:3661–4. [PubMed: 22127688]
5. Belot A, Cimaz R. Monogenic forms of systemic lupus erythematosus: new insights into SLE pathogenesis. Pediatr Rheumatol Online J. 2012; 10:21. [PubMed: 22883345]
6. Botto M, Kirschfink M, Macor P, Pickering MC, Wurzner R, Tedesco F. Complement in human diseases: lessons from complement deficiencies. Mol Immunol. 2009; 46:2774–83. [PubMed: 19481265]
7. Briggs TA, Rice GI, Daly S, Urquhart J, Gornall H, Bader-Meunier B, et al. Tartrate-resistant acid phosphatase deficiency causes a bone dysplasia with autoimmunity and a type I interferon expression signature. Nat Genet. 2011; 43:127–31. [PubMed: 21217755]
8. Lausch E, Janecke A, Bros M, Trojandt S, Alanay Y, De Laet C, et al. Genetic deficiency of tartrate-resistant acid phosphatase associated with skeletal dysplasia, cerebral calcifications and autoimmunity. Nat Genet. 2011; 43:132–7. [PubMed: 21217752]
9. Lee-Kirsch MA, Gong M, Chowdhury D, Senenko L, Engel K, Lee YA, et al. Mutations in the gene encoding the 3′–5′ DNA exonuclease TREX1 are associated with systemic lupus erythematosus. Nat Genet. 2007; 39:1065–7. [PubMed: 17660818]
10. Al-Mayouf SM, Sunker A, Abdwani R, Abrawi SA, Almurshedi F, Alhashmi N, et al. Loss-of-function variant in DNASE1L3 causes a familial form of systemic lupus erythematosus. Nat Genet. 2011; 43:1186–8. [PubMed: 22019780]
11. Anolik JH. B cell biology and dysfunction in SLE. Bull NYU Hosp Jt Dis. 2007; 65:182–6. [PubMed: 17922667]
12. Meffre E, Wardemann H. B-cell tolerance checkpoints in health and autoimmunity. Curr Opin Immunol. 2008; 20:632–8. [PubMed: 18848883]
13. Dorner T, Giesecke C, Lipsky PE. Mechanisms of B cell auto-immunity in SLE. Arthritis Res Ther. 2011; 13:243. [PubMed: 22078750]
14. Wu J, Wilson J, He J, Xiang L, Schur PH, Mountz JD. Fas ligand mutation in a patient with systemic lupus erythematosus and lymphoproliferative disease. J Clin Invest. 1996; 98:1107–13. [PubMed: 8787672]

15. Steinberg SF. Distinctive activation mechanisms and functions for protein kinase C*δ*. Biochem J. 2004; 384:449–59. [PubMed: 15491280]
16. Mecklenbrauker I, Saijo K, Zheng NY, Leitges M, Tarakhovsky A. Protein kinase C*δ* controls self-antigen-induced B-cell tolerance. Nature. 2002; 416:860–5. [PubMed: 11976686]
17. Miyamoto A, Nakayama K, Imaki H, Hirose S, Jiang Y, Abe M, et al. Increased proliferation of B cells and auto-immunity in mice lacking protein kinase C*δ*. Nature. 2002; 416:865–9. [PubMed: 11976687]
18. Tan EM, Cohen AS, Fries JF, Masi AT, McShane DJ, Rothfield NF, et al. The 1982 revised criteria for the classification of systemic lupus erythematosus. Arthritis Rheum. 1982; 25:1271–7. [PubMed: 7138600]
19. Andre J, Cimaz R, Ranchin B, Galambrun C, Bertrand Y, Bouvier R, et al. Overexpression of the antiapoptotic gene Bfl-1 in B cells from patients with familial systemic lupus erythematosus. Lupus. 2007; 16:95–100. [PubMed: 17402365]
20. Lee J, Kuchen S, Fischer R, Chang S, Lipsky PE. Identification and characterization of a human $CD5^+$ pre-naive B cell population. J Immunol. 2009; 182:4116–26. [PubMed: 19299709]
21. Newton AC. Protein kinase C: structural and spatial regulation by phosphorylation, cofactors, and macromolecular interactions. Chem Rev. 2001; 101:2353–64. [PubMed: 11749377]
22. Limnander A, Depeille P, Freedman TS, Liou J, Leitges M, Kurosaki T, et al. STIM1, PKC-*δ* and RasGRP set a threshold for proapoptotic Erk signaling during B cell development. Nat Immunol. 2011; 12:425–33. [PubMed: 21441934]
23. Jackson DN, Foster DA. The enigmatic protein kinase C*δ*: complex roles in cell proliferation and survival. FASEB J. 2004; 18:627–36. [PubMed: 15054085]
24. Grimaldi CM, Hicks R, Diamond B. B cell selection and susceptibility to autoimmunity. J Immunol. 2005; 174:1775–81. [PubMed: 15699102]
25. Picard C, McCarl CA, Papolos A, Khalil S, Luthy K, Hivroz C, et al. STIM1 mutation associated with a syndrome of immuno-deficiency and autoimmunity. N Engl J Med. 2009; 360:1971–80. [PubMed: 19420366]
26. Hu X, Kim H, Stahl E, Plenge R, Daly M, Raychaudhuri S. Integrating autoimmune risk loci with gene-expression data identifies specific pathogenic immune cell subsets. Am J Hum Genet. 2011; 89:496–506. [PubMed: 21963258]
27. Manjarrez-Orduno N, Marasco E, Chung SA, Katz MS, Kiridly JF, Simpfendorfer KR, et al. CSK regulatory polymorphism is associated with systemic lupus erythematosus and influences B-cell signaling and activation. Nat Genet. 2012; 44:1227–30. [PubMed: 23042117]

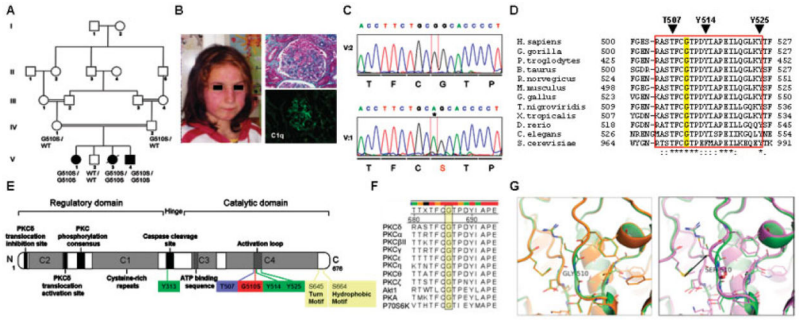

Figure 1.

Clinical features and genetics analyses. **A,** Pedigree of the consanguineous family in which 3 siblings have manifestations of systemic lupus erythematosus. Solid symbols represent affected individuals; open symbols represent unaffected individuals. The diagonal line indicates that the patient is deceased. **B,** Clinical and histologic characteristics of subject V-1. Left, Photograph of the patient shows a photosensitive cutaneous rash. Right, Biopsy sections of the kidney show World Health Organization classes IV–V lupus nephritis (top) and C1q deposits (bottom). **C,** Sequence trace of the G510 residue in subject V-2, the unaffected sibling with the homozygous wild-type (WT) allele, and in subject V-1, showing the homozygous nonsynonymous variant (c.1528G>A; p.G510S [★]). **D,** Sequence alignment of the activation loop (boxed area) of protein kinase Cδ (PKCδ) from vertebrates to yeast. **E,** Schematic representation of the structure of PKCδ, illustrating important functional domains. The relative positions of relevant phosphorylation sites are indicated. **F,** Conservation of the G510S residue (boxed area) in PKCδ and other members of the AGC family of protein kinases. **G,** Structural modeling of PKCδ G510S. Because the x-ray structure of PKCδ is unavailable, we modeled the G510S substitution in PKCδ using the homologous PKCθ. X-ray structures of PKCθ (green) are compared with the structures of wild-type PKCδ (orange) (left) and G510S PKCδ (purple) (right). Mutation to a serine residue causes disruption of the activation loop that houses the G510 residue (**thin black arrow**).

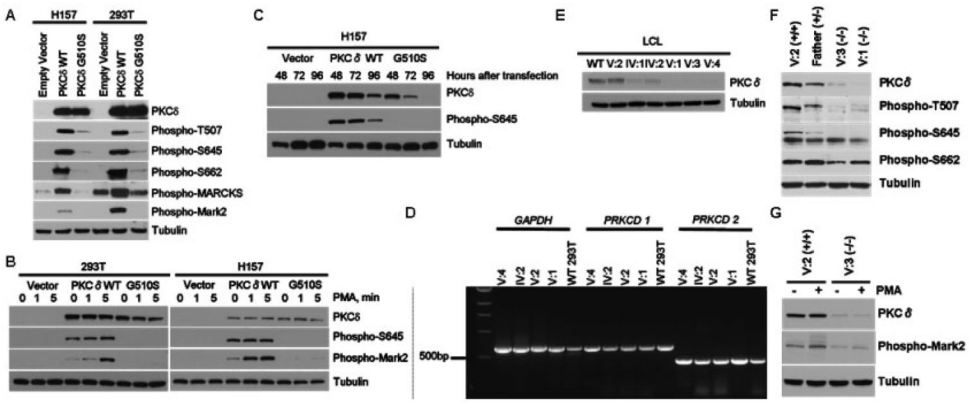

Figure 2.

Effect of the G510S mutation on the stability and function of PKC*δ*. **A,** Western blot showing weak phosphorylation of the T507, S645, and S662 sites in G510S PKC*δ*–transfected and wild-type PKC*δ*–transfected H157 and HEK 293T cells. Phosphorylation of the PKC*δ* substrates MARCKS and Mark2 was not increased by G510S. **B,** Western blot showing no induction of Mark2 phosphorylation in cells expressing G510S PKC*δ*, 5 minutes after phorbol myristate acetate (PMA) stimulation. **C,** Expression of wild-type PKC*δ* and G510S PKC*δ* constructs after transfection. Wild-type PKC*δ* expression persisted for up to 96 hours posttransfection, while the G510S mutant was undetectable at 96 hours and displayed significantly decreased levels at 72 hours. **D,** Effect of the G510S mutation on *PRKCD* mRNA integrity. Reverse transcription–polymerase chain reaction was performed to detect *PRKCD* and *GAPDH* in RNA extracted from lymphoblastoid cell lines (LCLs) established from affected siblings V-4 and V-1, their father (IV-2), and unaffected sibling (V-2) and from HEK 293T cells. **E** and **F,** Western blot analyses of LCL lysates harvested from family members, showing that patients with the G510S mutation express lower levels of PKC*δ* and reduced phosphorylation at the T507, S645, and S662 sites. **G,** Effect of PMA stimulation of LCLs from subjects V-2 and V-3. Stimulation did not induce PKC*δ* activation in homozygous patient V-3. See Figure 1 for other definitions.

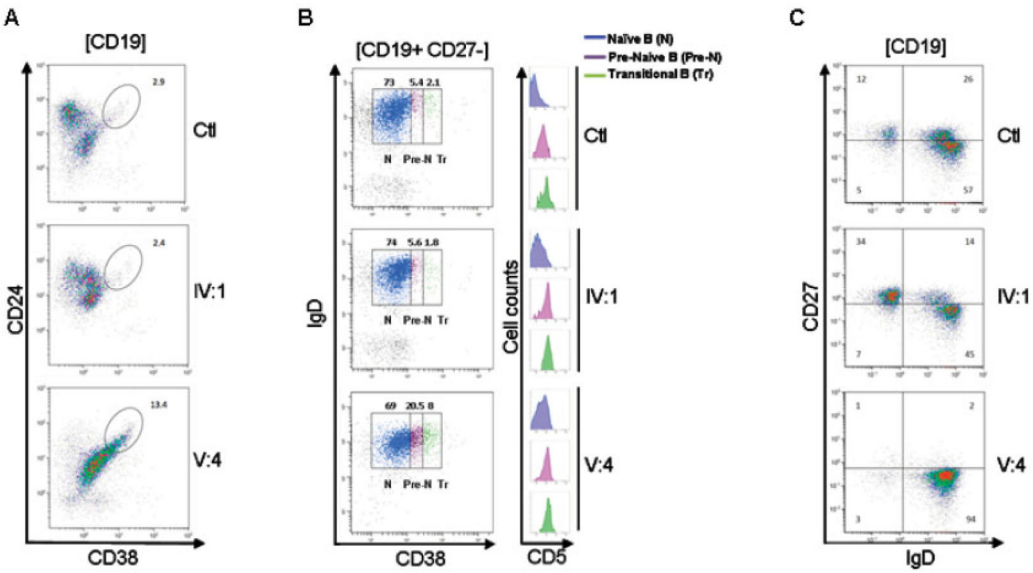

Figure 3.

Fluorescence-activated cell sorting (FACS) analysis of B cell subsets. **A,** Representative FACS plots showing increased percentages of transitional B cells in peripheral blood mononuclear cells isolated from subject V-4 (an affected sibling) but not in those obtained from either healthy donors (Ctl) or subject IV-1 (his heterozygous carrier mother). Transitional B cells were defined, according to the results of flow cytometry, as the $CD24^{high}CD38^{high}$ population within CD19+ cells. **B,** Assessment of CD5 expression by naive ($CD19+CD27-CD38^{low}IgD+$), pre-naive ($CD19+ CD27-CD38^{intermediate}IgD+$), and transitional ($CD19+CD27-CD38^{high}IgD+$) B cells from healthy donors, subject IV-1, and subject V-4. **C,** Decreased numbers of CD19+CD27+IgD+ and CD19+CD27+IgD− memory B cells in subject V-4 but not in healthy donors or subject IV-1. The percentage of IgD −CD27− memory B cells was unchanged, while the percentage of IgD+CD27− naive B cells was strongly increased, in subject V-4.

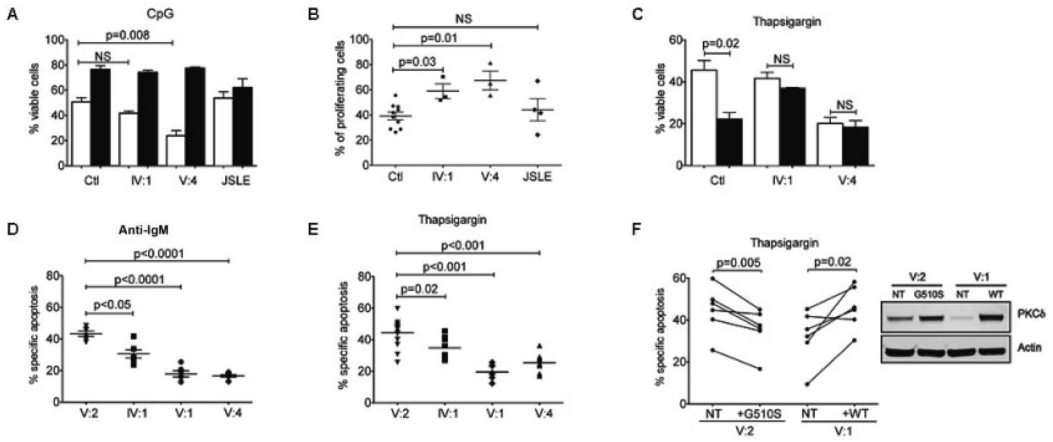

Figure 4.

Functional characterization of mutation and phenotype reversal. **A,** Percentage of viable CD19+ B cells isolated from wild-type (WT) healthy donors (Ctl), subject V-4, his mother (IV-1), and wild-type patients with juvenile-onset systemic lupus erythematosus (JSLE). B cells were cultured for 24 hours in the presence of medium alone (open bars) or the Toll-like receptor 9 ligand CpG (solid bars). Values are the mean ± SEM (n = 16 healthy donors, 3 patients with juvenile-onset SLE, and 3 independent samples each from subjects IV-1 and V-4). **B,** Proliferation of CD19+ B cells in response to anti-IgM, CD40L, and CpG stimulation of B cells from healthy donors, subjects V-4 and IV-1, and patients with juvenile-onset SLE. Values are the mean ± SEM (n = 10 healthy donors, 4 patients with juvenile-onset SLE, and 3 independent samples each from subjects IV-1 and V-4). **C,** Percentages of viable CD19+ B cells isolated from wild-type healthy donors and subjects V-4 and IV-1 after culturing for 24 hours in the presence of medium alone (open bars) or thapsigargin (solid bars). Values are the mean ± SEM (n = 10 healthy donors and 2 independent samples each from subjects IV-1 and V-4. **D** and **E,** Percentages of specific apoptosis of lymphoblastoid cell lines established from subjects V-1, V-2, V-4, or IV-1 following culturing for 24 hours in the presence of anti-IgM (**D**) or thapsigargin (**E**). Statistical analyses were performed using analysis of variance with Dunnett's correction. Symbols represent individual data points; horizontal lines and error bars show the mean ± SEM (n = 6–9 independent experiments each). **F,** Left, Percentages of specific apoptosis of LCLs established from subjects V-2 and V-1 that were either nontransduced (NT) or were transduced with protein kinase Cδ (PKCδ) G510S mutant construct (left) or PKCδ wild-type construct (right) and cultured for 24 hours with thapsigargin. Right, Western blot showing PKCδ expression in the corresponding LCLs. Results for transduced and nontransduced LCLs were compared by paired 2-tailed *t*-test. NS = not significant.

Table 1

Characteristics of the patients with PKCδ deficiency*

Subject	V-1	V-3	V-4	IV-1
Age at sampling, years	24	8	13	44
Sex	Female	Female	Male	Female
PRKCD mutation(s)	G510S/G510S	G510S/G510S	G510S/G510S	WT/G510S
Clinical manifestations				
Autoimmune disorder/SLE features	Skin involvement, alopecia, lupus nephritis, arthritis, neurologic involvement, dsDNA antibodies, ANAs, low C3 and C4	Skin involvement, autoimmune anemia, thrombocytopenia, antiphospholipid syndrome, lupus nephritis, CNS vasculitis, dsDNA antibodies, ANAs, low C3 and C4	Lupus nephritis, dsDNA antibodies, ANAs	None
Lymphoproliferative disease	Hepatomegaly	Lymphadenopathy, hepatosplenomegaly	None	None
Followup data	Chronic cutaneous lupus, CNS vasculitis, chronic renal failure	Death age 13 years (septic shock pseudomonas)	Asymptomatic with treatment	Asymptomatic
Immunologic features				
Lymphocyte count/μl (normal range)	1,073 (1,270–3,230)	778 (2,000–2,700)	1,861 (1,400–4,170)	2,714 (1,270–3,230)
T cell population, % (normal range)	21 (28–39)	9 (36–43)	32 (30–43)	31 (28–39)
CD3+	91 (61–80)	82 (65–80)	70 (59–77)	83 (61–80)
CD4+	53 (33–52)	46 (30–45)	41 (29–45)	51 (33–52)
CD8+	40 (21–40)	34 (19–43)	27 (20–45)	45 (20–45)
CD4+CD45RA+	ND	31 (55–67)	49 (55–67)	ND
CD4+CD25+CD127−	10 (4–10)	ND	4.4 (4–10)	ND
Natural killer CD56+CD16+ cells, % (normal range)	3 (8–25)	10 (8–25)	19 (10–23)	8 (9–18)
CD19+ B cells, % (normal range)	4 (9–18)	5 (10–20)	19 (10–23)	8 (9–18)
Immature B cells, CD19+CD21−	49 (9–18)	ND	20 (0–10)	7 (9–18)
Naive B cells, CD19+CD273IgD+	ND	ND	93 (43–87)	55 (43–87)
Memory B cells, CD19+CD27+	ND	ND	2 (14–46)	42 (14–46)
T cell proliferation after stimulation $\times 10^{-3}$ cpm (normal threshold)				
With concanavalin A	12 (>10)	Normal	81 (>10)	ND
With PMA	36 (>10)	Normal	88 (>10)	ND
With antigen		Normal	ND	ND
Tuberculin	23 (>10)	Normal	ND	ND
Candidin	71 (>10)	Normal	ND	ND
Immunoglobulin, gm/liter (normal range)				
IgG	10.4 (6.78–12.6)	12.10 (6.65–12.3)	11.2 (6.62–12.29)	ND
IgA	3.43 (0.75–2.38)	0.69 (0.51–1.63)	1.04 (0.6–1.9)	ND

Subject	V-1	V-3	V-4	IV-1
IgM	1 (0.71–2.02)	1.27 (0.51–1.63)	0.8 (0.53–1.53)	ND

* All thresholds and ranges are adjusted for age.

PCKδ; = protein kinase Cδ; SLE = systemic lupus erythematosus; dsDNA = double-stranded DNA; ANAs = antinuclear antibodies; CNS = central nervous system; ND = not done; PMA = phorbol myristate acetate.